

# Wind Farm Reactive Support and Voltage Control

Daniel F. Opila

Abdi M. Zeynu

Ian A. Hiskens

**Abstract**—Wind farms typically contain a variety of voltage control equipment including tap-changing transformers, switched capacitors, SVCs, STATCOMs, and the generators themselves. This paper focuses on the control of this equipment by addressing three major issues. The first is the ability of wind turbines to provide reactive power; voltage saturation in the collector system often limits the reactive power output of individual generators. The second topic is the stability of the system when independent control laws for the various types of equipment interact. Specifically, under some conditions a tap-changing transformer may not behave as expected or become unstable. The third major issue is the high-level control of the substation or wind farm; it is desirable to treat all the equipment as an integrated system rather than independent devices in order to meet cost, maintenance, fault tolerance, or other requirements. This high-level control problem is addressed for several types of available future information including exact future knowledge and stochastic predictions. Deterministic and Stochastic Dynamic Programming are used to develop control algorithms. The results demonstrate that while exact future knowledge is very useful, simple prediction methods yield no benefit.

## I. INTRODUCTION

UTILITY-SCALE wind generation facilities should be capable of regulating voltage through the provision of dynamic reactive support [1]. Wind farms, however, are comprised of many distributed [2] wind turbine generators (WTGs) and therefore exhibit behavior that is vastly different to that of traditional large generators. Nevertheless, from a power system operational point-of-view, wind farms should offer voltage controllability that is consistent with other forms of generation.

The voltage regulating capability of WTGs varies with generator technology and manufacturer [3]. Type 1 and 2 WTGs are based on induction generators, and have no inherent voltage controllability. Type 3 and 4 WTGs involve power electronic converters, which offer the ability to regulate reactive power, and hence achieve voltage control. For various reasons, this capability is often not utilized in type 3 WTGs. Rather, they are often operated at unity power factor. When reactive power regulation is enabled, WTG reactive power setpoints are usually coordinated by a central controller that determines a desirable schedule for all WTGs within the wind farm.

Wind generation installations typically contain a substation at the grid interconnection. These substations typically use

Research supported by the Department of Energy through award DE-EE0001382.

Daniel F. Opila, Abdi M. Zeynu and Ian A. Hiskens are with the University of Michigan, Ann Arbor, MI 48105 (e-mail: [dopila,mzeynu,hiskens]@umich.edu).

This material is based upon work supported under a National Science Foundation Graduate Research Fellowship. Daniel F. Opila was supported by NDSEG and NSF-GRFP fellowships.

a variety of equipment to regulate voltage: capacitors, tap-changing transformers, STATCOMs, SVCs, etc. The interactions between these systems can be difficult to predict. The system operator desires to use this equipment in the most efficient way possible to meet requirements and often has multiple conflicting goals.

This paper is a combination of three different ideas, all related to reactive power control. We first study the ability of WTGs to provide reactive power support and demonstrate that voltage limits in the collection grid limit the total amount of reactive power supplied. The available reactive power at the collector bus is often much less than the specified capability.

We next study the the stability of the system under a typical implementation: each device has its own independent controller. These independent control laws can interact to create unexpected or unstable behavior, especially with a tap-changing transformer as demonstrated here. This problem is addressed analytically for a simple system to generate threshold criteria for acceptable behavior.

The third major issue is the high-level long-term control of the substation or wind farm; it is desirable to treat all the equipment as an integrated system rather than independent devices in order to meet cost, maintenance, fault tolerance, or other requirements. This strategic control updates slowly (minutes) and involves some type of planning for the hours or days ahead. This is a challenging problem because the optimal decisions are time-dependent. Both the current state of the system and the future demands and requirements must be known to arrive at an optimal solution. Controllers are designed with various levels of future information to study of relative importance of forecasting and future estimation. Deterministic and Stochastic Dynamic Programming are used to develop optimal control algorithms.

This paper is organized as follows: Section II describes an example wind farm used in the analysis. Section III studies the amount of reactive power the WTGs can transmit to the collector bus. Section IV develops an analytical threshold when the voltage gain of a tap-changing transformer will unexpectedly change sign, that is, when increasing the tap ratio will decrease the high-side voltage. Section V analyzes the case where interactions between a tap-changing transformer and a reactive current source can cause instability. Section VI studies the substation-level control problem of controlling all the equipment to meet high-level long term goals. Finally, conclusions are presented in Section VII.

## II. SYSTEM LAYOUT AND PROBLEM MOTIVATION

A schematic layout of a generic wind farm is depicted in Figure 1. Turbines typically have some form of shunt compensation and a step-up transformer (buses 4 and 5)

connecting to a collector system (L3) that transmits power to a substation (buses 2 and 3). Many turbines are connected through a single substation, which typically contains switched capacitors for passive reactive power support, as well as active reactive support in the form of SVCs or STATCOMs. A step-up tap-changing transformer T2 connects the substation to the power grid and the infinite bus 1.

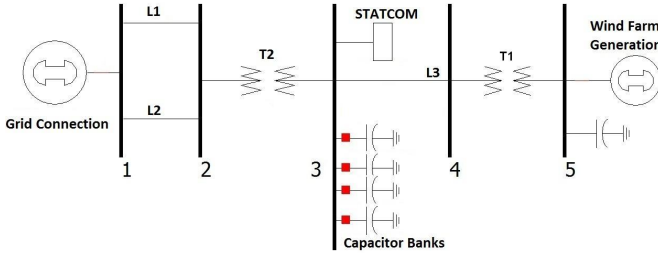


Fig. 1: A generic wind farm layout.

The equipment on buses 2 and 3 are physically located in the same substation to provide overall reactive power support for the wind farm.

While the overall layout of the wind farm is shown in Figure 1, the following sections will focus on particular aspects of the problem and will make simplifying assumptions. Section III analyzes the collector grid, and Sections IV-VI focus on the substation. Each section will specify the particular model under consideration.

### III. COLLECTOR SYSTEM IMPACT ON REACTIVE POWER AVAILABILITY

Type 3 and 4 WTGs employ power electronic converters that allow production or absorption of reactive power. Many WTGs, for example, are capable of operating over a power factor range of 0.95 lagging (generating reactive power) to 0.95 leading (absorbing reacting power) at full active power output. Manufacturers specify active/reactive capability curves for their WTGs to describe their exact operational characteristics. Often wind farm developers use those capability curves directly to determine the total reactive power available at the point of interconnection. Whilst such calculations take into account losses on the collector system, they tend not to consider voltage rises/falls across the collector feeders and WTG step-up transformers. The following discussion shows that as a result, the total reactive power (both lagging and leading) that's available at the collector bus tends to be overstated.

In discussing the restrictions on reactive power that arise due to collector bus voltages, it is convenient to refer to the example system shown in Figure 2. For clarity, the figure does not show the step-up transformers associated with each WTG, though those transformers have been included in the analysis. Also, the discussion focuses on reactive power production (WTGs operating in lagging power factor), though a similar argument holds for reactive power absorption (leading power factor).

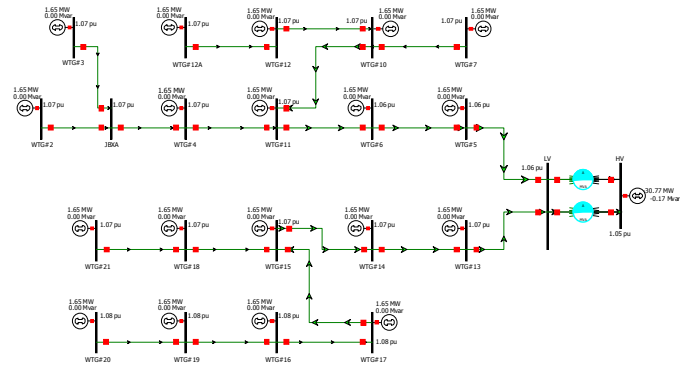


Fig. 2: Example wind farm topology.

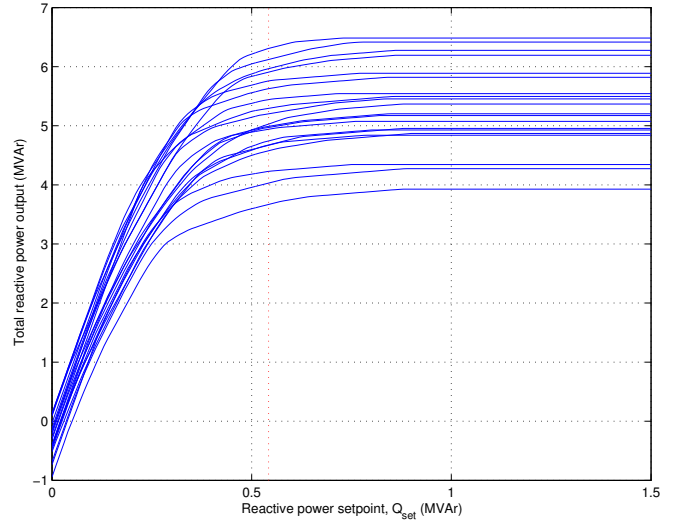


Fig. 3: Variation of total reactive power with setpoint  $Q_{set}$ .

Consider a process where the reactive power output from all WTGs is increased simultaneously. This could be achieved by a central controller sending every WTG a reactive power setpoint  $Q_{set}$ . With  $Q_{set} = 0$ , none of the WTGs would be at their voltage limits, so all could respond to a change in the setpoint  $\Delta Q_{set}$ . The example system consists of 19 WTGs, so the total change in reactive power supplied to the collector bus would be approximately  $19 \times \Delta Q_{set}$ . (Losses would change by a small amount.) As  $Q_{set}$  increases, voltages across the collector system will increase, with the most dramatic increases occurring at the remote ends of radial feeders. Eventually those WTGs at the ends of feeders will encounter their upper voltage limits. To ensure the voltage limit is not exceeded, protection overrides the  $Q_{set}$  setpoint. Reactive power output can no longer increase with increasing  $Q_{set}$ , and in fact may fall to ensure the voltage does not rise above the limit. As  $Q_{set}$  continues to increase, more and more WTGs will reach their upper voltage limits, preventing further increase in their reactive power output.

The process described above was simulated using a continuation power flow. Results of this process, for the example system of Figure 2, are shown in Figure 3. Each curve in the figure corresponds to a different, randomly chosen, set of active power generation values for the WTGs. It can be

seen that the reactive power output saturates in every case. For small  $Q_{set}$ , the slope of each curve is close to 19, the number of WTGs. However, as  $Q_{set}$  increases, and WTGs progressively encounter their voltage limits, the slope steadily decreases. Eventually all WTGs are on voltage limits, and further increases in  $Q_{set}$  have no effect.

For this example, all WTGs are rated to produce 1.65 MW at 0.95 power factor (lagging and leading), which corresponds to maximum reactive power of 0.54 MVar. This suggests the WTGs should be capable of supplying total reactive power of around  $19 \times 0.54 = 10.3$  MVar. In fact, based on Figure 3, the maximum available reactive power is actually less than 6.5 MVar, and may be as low as 3.7 MVar. The restriction is due to each WTG's upper voltage limit of  $V_{max} = 1.1$  pu.

Wind farms that include long radial feeders are most prone to saturation in total reactive power output. The effect is less significant for short feeders. Clearly, the collector system topology must be taken into account when assessing the total reactive power available from WTGs.

#### IV. TRANSFORMER TAP-CHANGING GAINS

##### A. Background

It is not uncommon for step-up transformers associated with traditional generators to be used to regulate their high-side bus voltage. In a similar way, numerous wind farms have sought to use the tap-changing capability of their collector transformers to regulate the voltage at the (high voltage) point of interconnection. In many cases, tap changing frequently exhibits unstable behavior, with the transformer tapping to an upper or lower limit and remaining there. Consequently, tapping-based voltage regulation is often disabled.

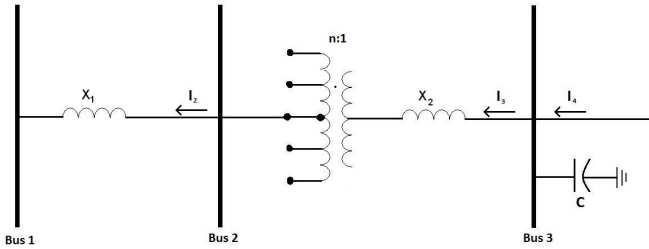


Fig. 4: Power system for analyzing tap-changing dynamics.

In the following analysis, the simple power system of Figure 4 will be used to explore the nature of tap-changing instability, and to suggest sufficient conditions for ensuring stable behavior. Given the tapping arrangement shown in Figure 4, the voltage regulator requires  $\frac{dV_2}{dn} > 0$  for correct operation, i.e., it is assumed that an increase in tap raises the voltage on the high-voltage (tapped) side of the transformer. The following analysis shows that such a condition is not always satisfied.

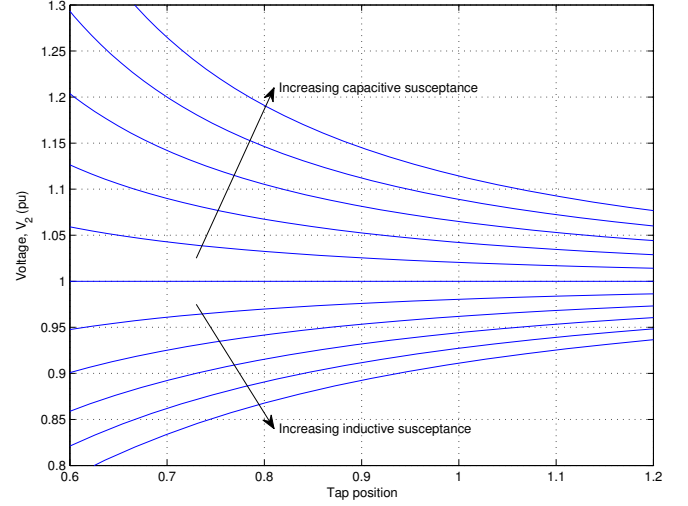


Fig. 5: Curves of  $V_2$  versus  $n$  for various values of capacitive and inductive susceptance.

##### B. Passive voltage support

Initially consider the case where the wind farm has zero output, and the only device connected to the collector bus is a capacitor  $C$ . The injected current is given by

$$I_3 = -jBV_3$$

where  $B = \omega C$  is the capacitive susceptance. Simple circuit analysis yields

$$V_2 = \frac{1}{1 - \frac{X_1 B}{n^2(1 - BX_2)}} \times V_1. \quad (1)$$

In per unit, it is normal for  $BX_2 \ll 1$ . This allows (1) to be simplified, giving

$$V_2 = \frac{1}{1 - \frac{X_1 B}{n^2}} \times V_1. \quad (2)$$

Assuming constant susceptance  $B$ , differentiating gives

$$\frac{dV_2}{dn} = -\frac{2nX_1BV_1}{(n^2 - X_1B)^2}. \quad (3)$$

With capacitance connected to the collector bus, susceptance  $B$  is positive. It follows that  $\frac{dV_2}{dn} < 0$ , implying that tap changing is unstable. Capacitance is commonly connected to the collector bus to provide power factor correction and reactive support. Furthermore, when a Static VAR Compensator (SVC) is at its capacitive limit, it is effectively just a capacitor.

Notice that if shunt reactors (inductors) are connected to the collector bus, then the susceptance becomes  $B = -\frac{1}{\omega L}$ . According to (3),  $\frac{dV_2}{dn} > 0$  in this case. It follows that the tap changer would operate correctly to achieve voltage regulation. Figure 5 shows plots of  $V_2$  versus tap position  $n$  for the system shown in Figure 4, with various levels of capacitive and inductive susceptance. The slopes of the curves are in agreement with (3).

The simplified analysis above assumed zero active power production from the WTGs. To explore this effect, active power of 1.0 pu, at unity power factor, was injected by the

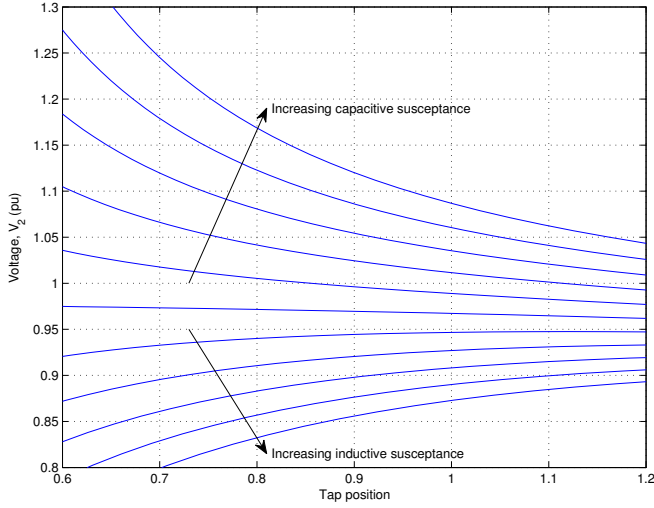


Fig. 6: Curves of  $V_2$  versus  $n$  taking into account WTG active power production.

WTGs into the collector bus. The continuation power flow cases of Figure 5 were repeated with this power injection, and are shown in Figure 6. Notice that the conclusions drawn in the prior analysis remain true:

$$\begin{aligned} \text{capacitive susceptance} &\Rightarrow \frac{dV_2}{dn} < 0 \\ \text{inductive susceptance} &\Rightarrow \frac{dV_2}{dn} > 0. \end{aligned}$$

When STATCOMs encounter a limit, they act as a current source. It is therefore useful to consider the case of a reactive current source

$$I_3 = j\hat{I}_3 \quad (4)$$

injecting current into the collector bus. Note that  $\hat{I}_3 > 0$  for an inductive source (reactive power delivered from the grid to the STATCOM), with  $\hat{I}_3 < 0$  for a capacitive source (reactive power delivered from the STATCOM to the grid.) Again, simple circuit analysis yields

$$V_2 = V_1 - X_1 \frac{\hat{I}_3}{n} \quad (5)$$

and so

$$\frac{dV_2}{dn} = X_1 \frac{\hat{I}_3}{n^2}.$$

If the current source is inductive,  $\frac{dV_2}{dn} > 0$  and hence tapping-based voltage regulation will operate correctly. However, if the current source is capacitive,  $\frac{dV_2}{dn} < 0$ , so tap-changer control will go unstable. The continuation power flows of Figure 5 were repeated for these current injection cases, with the results shown in Figure 7.

### C. Active voltage support

Consider a reactive support device that injects voltage dependent current

$$I_3(V_3) = j\hat{I}_3(V_3)$$

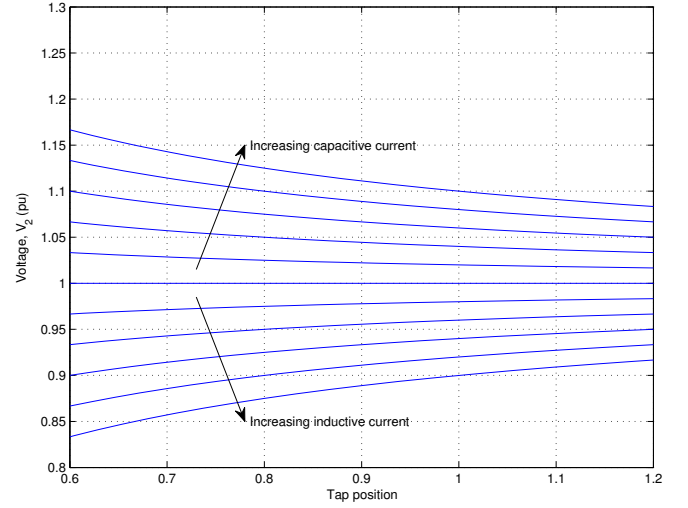


Fig. 7: Curves of  $V_2$  versus  $n$  for various values of capacitive and inductive current injection.

into the collector bus. It can be shown that in this general case,  $\frac{dV_2}{dn}$  takes the form

$$\frac{dV_2}{dn} = \frac{\hat{I}_3(V_3) + V_3 \frac{d\hat{I}_3(V_3)}{dV_3}}{\frac{n^2}{X_1} + \frac{d\hat{I}_3(V_3)}{dV_3}}. \quad (6)$$

In the special case where reactive support is provided by a capacitor, we have

$$\hat{I}_3(V_3) = -BV_3. \quad (7)$$

Substituting this into (6) and simplifying gives (3), as expected. The advantage of (6), though, is that more general forms of support may be considered.

1) *STATCOMs*: Assume a STATCOM has current limits of  $\pm \bar{I}_{stat}$ . (Recall the current convention of Figure 4, which implies capacitive current is negative.) It is common for voltage control to employ a droop characteristic, such that the current injected into the collector bus is given by,

$$I_{stat} = \frac{\bar{I}_{stat}}{D_{stat}} (V - \bar{V}) \quad (8)$$

where  $D_{stat}$  is the droop value (typically around 0.03-0.05),  $\bar{V}$  is the target voltage at zero output, and  $V$  is the collector bus voltage. This yields full output when the voltage difference exceeds the droop value. All quantities are in per unit.

With a fixed capacitor and a STATCOM at the collector bus, the total injected current is,

$$\hat{I}_3(V_3) = -BV_3 + \frac{\bar{I}_{stat}}{D_{stat}} (V_3 - \bar{V}), \quad (9)$$

and hence

$$\frac{d\hat{I}_3(V_3)}{dV_3} = -B + \frac{\bar{I}_{stat}}{D_{stat}}. \quad (10)$$

From (6), positive (stable)  $\frac{dV_2}{dn}$  requires that

$$\hat{I}_3(V_3) + V_3 \frac{d\hat{I}_3(V_3)}{dV_3} > 0. \quad (11)$$

Substituting (9) and (10) into (11) and simplifying gives

$$-2BV_3 + \frac{\bar{I}_{stat}}{D_{stat}}(2V_3 - \bar{V}) > 0.$$

Exploiting the fact that  $V_3 \approx \bar{V}$  allows further simplification,

$$\frac{\bar{I}_{stat}}{D_{stat}} > 2B. \quad (12)$$

For a capacitor,  $B > 0$ , implying  $D_{stat} > 0$ . Therefore,  $\frac{dV_2}{dn}$  will be positive if

$$0 < D_{stat} < \frac{\bar{I}_{stat}}{2B}. \quad (13)$$

It is interesting that the STATCOM droop characteristic must over-compensate the capacitor to ensure  $\frac{dV_2}{dn} > 0$ . To explore this result further, consider the situation if the droop characteristic only just compensated the fixed capacitor, i.e.,  $\frac{\bar{I}_{stat}}{D_{stat}} = B$ . According to (9), the net current injection would be

$$\hat{I}_3(V_3) = -B\bar{V}, \quad (14)$$

which is effectively a constant capacitive current. It was shown in Figure 7, though, that  $\frac{dV_2}{dn} < 0$  for such a current injection. By requiring the condition (12), the inductive effect of the droop characteristic overcomes the combined effects of the actual capacitor and the ‘‘apparent’’ capacitive current source (14).

2) *SVCs*: SVCs introduce a variable susceptance  $B$  into the current injection equation (7). With  $B$  functionally dependent upon  $V_3$ , the derivative  $\frac{d\hat{I}_3}{dV_3}$  becomes,

$$\frac{d\hat{I}_3}{dV_3} = -B - V_3 \frac{dB}{dV_3}. \quad (15)$$

Substituting (7) and (15) into (11) gives,

$$\begin{aligned} -BV_3 - V_3\left(B + V_3 \frac{dB}{dV_3}\right) &> 0 \\ \Rightarrow 2B + V_3 \frac{dB}{dV_3} &< 0 \\ \Rightarrow \frac{dB}{dV_3} &< -\frac{2B}{V_3}. \end{aligned} \quad (16)$$

Assume an SVC has symmetric susceptance limits  $\pm\bar{B}_{svc}$ , where capacitive susceptance is positive. A typical droop characteristic has the form

$$B_{svc} = \frac{\bar{B}_{svc}}{D_{svc}}(\bar{V} - V) \quad (17)$$

where parameters are defined similarly to (8), and are again in per unit. If a fixed capacitor with susceptance  $-B_{fix}$  is connected to the collector bus together with the SVC, then the total susceptance is

$$B(V_3) = B_{fix} + B_{svc}(V_3),$$

and

$$\frac{dB(V_3)}{dV_3} = -\frac{\bar{B}_{svc}}{D_{svc}}.$$

It follows from (16) that  $\frac{dV_2}{dn}$  is positive (stable) when

$$\frac{\bar{B}_{svc}}{D_{svc}} > \frac{2B}{V_3}.$$

To ensure this condition is satisfied over the full range of  $B(V_3)$  requires that

$$\frac{\bar{B}_{svc}}{D_{svc}} > \frac{2(B_{fix} + \bar{B}_{svc})}{V_3},$$

or rewriting,

$$0 < D_{svc} < \frac{V_3\bar{B}_{svc}}{2(B_{fix} + \bar{B}_{svc})}.$$

## V. TRANSFORMER TAP-CHANGING DYNAMICS

This section addresses a similar issue to Section IV, but now considers the system dynamics rather than the steady-state condition. The results derived in Section IV are ‘‘static’’ in that they do not depend on time or the previous states of the system. There are no functions of time or time derivatives.

Now, we consider the case where the tap-changing and voltage support controllers have their own dynamics. Specifically, the controllers for tap-changing and reactive support are single input single output (SISO) integral controllers that operate independently, as is typically the case when control is isolated on each particular piece of hardware.

The main consideration is the relative speed between the two control loops. We will show that if the tap-changing controller is sufficiently fast (aggressive) compared to the reactive support, it can cause instability.

Using the same system considered in Section IV and shown in Figure 4, we assume a reactive current injection into the collector bus as in (4).  $V_2$  is given by (5) and  $V_3$  is

$$V_3 = \frac{V_1}{n} - X \frac{\hat{I}_3(V_3)}{n^2}. \quad (18)$$

Let target voltages (set by the operator) at bus 2 and 3 be  $\bar{V}_2$  and  $\bar{V}_3$ . For simplicity, assume that continuous tap ratios are available. Then the independent SISO integral controllers for the tap ratio  $n$  and the reactive power injection  $\hat{I}_3$  are

$$\dot{n} = -k_n(V_2 - \bar{V}_2) \quad (19)$$

$$\dot{\hat{I}}_3 = (V_3 - \bar{V}_3). \quad (20)$$

Normally, the speed of each control loop would be scaled by some gain. In this case, we are primarily interested in stability and the important factor is the *relative* speed between the two loops. Therefore, the gains are normalized by the gain of the reactive support loop (20), leaving it with a gain of one. The gain  $k_n$  (positive) in (19) represents the relative speed of the two loops; increasing  $k_n$  means the tap changing is becoming faster and more aggressive relative to the reactive support.

To check the stability of the system, we linearize the dynamics about an equilibrium point. For simplicity, let us assume that the desired set points are  $\bar{V}_3 = 1$ , and  $\bar{V}_2$  is a function of the equilibrium tap ratio  $\bar{n}$ . This leaves  $\bar{V}_2 = \bar{n}V_3$  (i.e.  $\bar{n} = 1.05$ ). At this equilibrium point, all derivatives will be zero and the system will remain there unless perturbed. Setting the derivatives (19) and (20) equal to zero and substituting (5) and (18),

$$\dot{n} = 0 = -k_n(V_1 - X \frac{\hat{I}_3(V_3)}{n} - \bar{V}_2) \quad (21)$$

$$\dot{\hat{I}}_3 = 0 = (\frac{V_1}{n} - X \frac{\hat{I}_3(V_3)}{n^2} - \bar{V}_3). \quad (22)$$

An important distinction is the difference between a state ( $n$  or  $V_2$ ) and the linearization point ( $\bar{n}$  or  $\bar{V}_2$ ). A fixed equilibrium point, denoted by a bar, is selected to conduct the linearization, but the system dynamics still evolve about that point.

Equations (21) and (22) are identical given our definition of  $\bar{V}_2$  and may be solved for the equilibrium current injection,

$$\hat{I}_3(V_3) = -\frac{n(\bar{n} - 1)V_1}{X} \quad (23)$$

completing our specification of the equilibrium point.

Taking the partial derivatives of (21) and (22), substituting (23) and assuming that  $V_1 = 1$  we are left with the linearized system dynamics

$$\begin{bmatrix} \dot{n} \\ \dot{\hat{I}}_3 \end{bmatrix} = \frac{1}{\bar{n}^2} \begin{bmatrix} k_n \bar{n}(\bar{n} - 1) & k_n \bar{n} X \\ 1 - 2\bar{n} & -X \end{bmatrix} \begin{bmatrix} \delta n \\ \delta \hat{I}_3 \end{bmatrix}, \quad (24)$$

which has a characteristic polynomial

$$s^2 + s(-k_n \bar{n}(\bar{n} - 1) + X) + \bar{n}^2 k_n X. \quad (25)$$

Given that the final term is positive by the definition of  $k_n$ , the  $s$  term must contain a positive coefficient to yield two stable eigenvalues. This condition holds when  $0 < \bar{n} < 1$  for positive  $X$ . However, when  $\bar{n} > 1$ , there is a maximum tap changing gain  $k_n$  to ensure stability,

$$k_n < \frac{X}{\bar{n}(\bar{n} - 1)}. \quad (26)$$

In short, if the bus 2 voltage setpoint  $\bar{V}_2$  is less than 1 p.u. ( $\bar{n} < 1$ ) there is no stability issue, but if not, a sufficiently aggressive tap changer can make the system go unstable.

## VI. SUPERVISORY CONTROL OF REACTIVE POWER SUPPORT

As previously discussed, reactive power may be controlled by a combination of capacitors, tap-changing transformers, and FACTS devices. The system operator desires to use this equipment in the most efficient way possible to meet requirements and often has multiple conflicting goals. For example, these goals may include minimizing capacitor switching, tap changing, and power losses while maximizing reactive reserve. More sophisticated objectives are possible, like prioritizing different kinds of reactive reserve (i.e. capacitors vs. STATCOMS) or maximizing the possibility of successfully dealing with a system fault. There is significant potential for better control performance by incorporating future knowledge, including wind and load forecasts.

This level of complexity suggests the need for a system-level control approach. Here we focus on the control of reactive power support, where all the reactive power sources are controlled by a single controller. This approach may yield

better performance than controllers simply based on individual devices. This section focuses on the long-term supervisory control which makes decisions at a relatively slower rate, roughly once per minute or slower. Fault conditions or fast transients are assumed to be handled by standard control methods.

### A. Problem Formulation

This system level control problem is treated as a dynamic optimization problem. An important aspect of this type of problem is the type of future information available, its quality, and the forecasting horizon. The goal here is to generate the best possible controller given the available information.

Consider an optimization problem with a finite horizon, even if very long, perhaps a year. We group the various types of future information into five broad classes:

- 1) **Exact Future Knowledge** - Exact knowledge of the future for the full time horizon. This yields the maximum attainable performance, although it is unrealistic in practice. A less restrictive case assumes that exact future knowledge is available, but only for a short duration, i.e. a 24-hour exact forecast.
- 2) **Uncertain Future Knowledge** - Time-dependent future information with uncertainty of some type, including uncertain forecasts and time-dependent markov transition probabilities. This information may be available for the full time horizon or a shorter duration.
- 3) **Cyclical Stochastic Knowledge** - General stochastic predictions about the future that are repetitive and cyclical. An example are markov transition probabilities that change based on the time of day, but are repeated each day. This category is well-suited to model daily demand fluctuations as well as day/night wind patterns.
- 4) **Stationary Stochastic Knowledge** - Stationary stochastic predictions about the future, including markov-chain based wind models. No explicit forecasting or time-dependent knowledge is required.
- 5) **No Explicit Future Knowledge** - Both optimization- and rule-based methods that do not explicitly account for the future.

Each of these five classes will generate controllers with different characteristics. Several controller subtypes are available for each class; the information class is identified for each controller type proposed in the following Section VI-B. The list is ordered roughly in decreasing order of complexity and performance. In general, having more information available is not guaranteed to improve performance, but it should do no worse than the baseline case. The two extreme cases (1 & 5) listed above may be undesirable, which forces the determination of the best tradeoff between performance and complexity. Specifically, the designer should determine the performance improvement available with increasing controller complexity in order to make an informed decision

1) *Overall Optimization Strategy*: The most general formulation describes the system dynamics using a function of the system state  $x$ , control input  $u$ , and disturbance  $w$ ,

$$x_{k+1} = f_k(x_k, u_k, w_k). \quad (27)$$

The function  $f$  may or may not change with time, as represented by  $f_k$ .

For a given time series of states ( $x_1 \dots x_T$ ), controls ( $u_1 \dots u_T$ ), and disturbances ( $w_1 \dots w_T$ ) a performance metric  $J$  is assigned to represent the total cost. A general optimization formulation represents this cost as a function  $\Phi$  that is of the states, controls, and disturbances over a time window  $T$ ,

$$J = \Phi(x_1 \dots x_T, u_1 \dots u_T, w_1 \dots w_T). \quad (28)$$

Other formulations are available that generate a finite cost even with infinite stopping time, for example by discounting future costs.

Many different techniques are available to solve these types of problems, but optimal solutions can be difficult to obtain because the number of possible control sequences grows exponentially with time. If the total cost is restricted to be an additive cost function  $c_k(x_k, u_k)$  that can be evaluated at each individual time step,

$$\sum_0^T c_k(x_k, u_k), \quad (29)$$

techniques are available to drastically reduce computation requirements. The subscript  $k$  denotes that the cost may be a function of time. We focus on problems of this type. Thus, the optimization problem may be stated formally as minimizing (29) subject to possibly time-dependent constraints  $g_k(x_k, u_k)$ ,

$$\begin{aligned} \min \sum_0^T c_k(x, u) \\ \text{such that} \\ g_k(x_k, u_k) \leq 0 \quad \forall k. \end{aligned} \quad (30)$$

In this work we generate test optimization-based controllers for three cases including the two extremes extreme cases: exact future knowledge, stationary stochastic knowledge, and no explicit future knowledge. In addition, these three controllers are compared to a “baseline” algorithm that uses hysteresis-based switching of the capacitors based on current reactive power demand.

2) *Example System*: To illustrate the control techniques presented here, a simple test system is studied. This system consists of a wind farm collector system connected to an infinite bus through a substation. The substation has four capacitor banks and a STATCOM for reactive power compensation, just as shown in Figure 1. The optimization goal is to minimize both STATCOM usage and capacitor switching. The STATCOM is assumed to perfectly regulate the bus voltage  $V_3$  and supply any reactive power not supplied by the capacitors. For now, the STATCOM is also assumed to have unlimited capability, but realistic limits may be easily implemented. This yields a relatively simple power flow problem, while clearly illustrating the control problem. The power flow equations are solved to determine the reactive power required to hold the bus at 1 V p.u., and the optimization is simply the distribution of this reactive power between the STATCOM and capacitors.

To model this system in terms of (30), the system has four states  $x$  representing the current state of each capacitor bank, either on or off. Four controls  $u$  represent the command to turn each capacitor bank on or off. Thus the system dynamics (27) reflect the simple result that at the next time step, the capacitor state  $x_{k+1}$  will match the current command  $u_k$ .

For the cost function, the number of capacitor switches  $N_{CS}$  is weighted by a penalty  $\alpha$  to reflect maintenance and wear costs. The STATCOM usage  $\bar{S}$  is calculated based on the current reactive power demand and the capacitance supplied by the control  $u_k$ .  $\bar{S}$  is defined as the time integral of STATCOM usage over the time step. We are interested in the relative tradeoff between capacitor switches and STATCOM usage and need only one tuning parameter, so  $\bar{S}$  has penalty one,

$$c_k(x_k, u_k) = \alpha N_{CS} + abs(\bar{S}). \quad (31)$$

These two definitions of  $c_k(x, u)$  and  $f_k(x, u)$  form the basic optimization problem and are used in the various algorithms.

## B. Control Design Methods for Various Information Classes

The control design methods proposed here are standard techniques. The main ideas are presented here, but full details are available in standard texts [4], [5].

1) *Deterministic Dynamic Programming*: In the case of exact future knowledge, Deterministic Dynamic Programming (DDP) is used to solve (30). For each time step, the optimal “cost to go” function  $J_k^*(x)$  is calculated. It represents the minimum cost required to go from time  $k$  and state  $x$  to the final time  $T$ . Starting at the final time  $T$ , the terminal cost (if any) is assigned for the final state, yielding  $J_T^*(x)$ . The algorithm proceeds by backward recursion,

$$J_k^*(x) = \min_{u \in U} [c_k(x, u) + J_{k+1}^*(f_k(x_k, u))], \quad (32)$$

where  $c(x, u)$  is the instantaneous cost as a function of state and control. Recall that the function  $f_k(x_k, u_k)$  determines the next state  $x_{k+1}$ . This equation represents a compromise between minimizing the current cost  $c_k(x, u)$  and the future cost  $J(x_{k+1})$ . This formulation is entirely deterministic with no stochastic disturbances because the exact future is known. Anything that changes with time, e.g. reactive power demand, is included in the time-varying cost  $c_k(x, u)$  or dynamics  $f_k(x_k, u_k)$ . In this case, the cost is given by (31) and changes based on the required reactive power.

The optimal control  $u^*$  is any control that achieves the minimum cost  $J_k^*(x)$  in (32),

$$u_k^*(x) = \operatorname{argmin}_{u \in U} [c(x_k, u) + J_k^*(f_k(x_k, u))]. \quad (33)$$

This method requires two steps: an off-line step to calculate the controller using the future knowledge, and an on-line step where the control is causally implemented, possibly in real-time. The off-line step solves (32), and the end result is a control policy  $u_k^*(x)$  and a cost-to-go  $J_k(x)$ , both for all times  $k$ . In the on-line implementation, one may either use the policy  $u_k^*(x)$  or calculate the control on-line using (33) and the cost-to-go  $J_k(x)$ . Intuitively,  $J_k(x)$  represents the minimum cost

required to operate from time  $k$  until time  $T$  when starting in state  $x$ . It essentially contains the future information about the system.

2) *Stochastic Dynamic Programming*: Stochastic Dynamic Programming (SDP) is used to incorporate uncertain future knowledge, stationary stochastic knowledge in this case. This algorithm is a variant of the deterministic version described previously, but the main ideas are the same. The key difference is that the future is uncertain, so everything is based on an expectation of the future  $E_w$  over the disturbance  $w$ . While the designer still wished to solve (30), the algorithm can no longer solve it exactly due to the uncertain future. Instead, the algorithm uses a slightly different optimization formulation,

$$\begin{aligned} \min E_w \sum_0^\infty \gamma^k c(x, u) \\ \text{such that} \end{aligned} \quad (34)$$

$$g(x, u) \leq 0 \quad \forall k. \quad (35)$$

This formulation differs from (30) in several ways. The future cost is discounted by the factor  $\gamma < 1$ , which keeps the sum finite. This technique is called “infinite horizon discounted future cost.” Although the time horizon is no longer finite, a value of  $\gamma$  close to one forces the algorithm to consider a “reasonable” time horizon, while discounting the infinite future.

To use the algorithm,

$$V^*(x) = \min_{u \in U} E_w [c(x, u) + V^*(f(x, u, w))] \quad (36)$$

is solved for the “Value Function”  $V(x)$ . The value function is very similar to the cost-to-go  $J_k(x)$  in (32). The primary difference is that  $V(x)$  is not a function of time, only the state. It represents the expected future cost of being in state  $x$ . The time horizon is infinite, and hence  $V(x)$  does not change with  $k$ . The optimal control  $u^*$  is again any control that achieves the minimum cost  $V^*(x)$  in (36),

$$u^*(x) = \operatorname{argmin}_{u \in U} E_w [c(x, u) + V^*(f(x, u, w))]. \quad (37)$$

The control policy is also independent of time and hence is a stationary policy.

The future disturbances, wind power in this case, are specified via a finite-state Markov chain rather than exact future knowledge. This wind model adds additional states to the model. In general, the designer must determine the probability distribution of the disturbance  $w$  based on the current state and control,

$$P(w_k | x_k, u_k). \quad (38)$$

In this paper we use a one state Markov chain. The current wind power  $P_k$  is the state, and the probability of the next wind power depends on the current wind power. This means estimating the function

$$P(P_{k+1} | P_k). \quad (39)$$

The designer may choose how this disturbance is specified. For example, the disturbance may be the next wind power, or

it may be the change in wind power. More complex models can be used by adding additional model states, perhaps the last three recorded wind powers.

The transition probabilities (39) are estimated from known wind patterns. The powers  $P$  are discretized to form a grid. For each discrete state  $P_k$  there are a variety of outcomes  $P_{k+1}$ . The probability of each outcome  $P_{k+1}$  is estimated based on its frequency of occurrence, and is a function of the current wind power.

3) *Instantaneous Optimization*: The simplest optimization-based algorithm seeks to minimize cost with no future knowledge. This technique is termed Instantaneous Optimization (IO) because it has no estimate or prediction of the future and the control is generated by minimizing the current cost at each instant,

$$u^*(x) = \operatorname{argmin}_{u \in U} c(x, u). \quad (40)$$

The control decision clearly lacks the future estimates of (33) and (37).

4) *Baseline Controller*: The baseline controller is not based on optimization at all, but a simple rule-based hysteresis. Recall that the STATCOM usage  $\bar{S}$  is the difference between the required reactive power and that supplied by the capacitors. A switching threshold  $\beta$  is assigned, and when the STATCOM usage exceeds this threshold, an additional capacitor bank is switched in or out. Define  $NC$  as the number of capacitor banks currently switched in. This leaves the update rule as

$$NC_{k+1} = \begin{cases} NC_k + 1 & \text{if } \bar{S} > \beta \\ NC_k - 1 & \text{if } \bar{S} < -\beta \\ NC_k & \text{otherwise.} \end{cases} \quad (41)$$

### C. Simulation Results

The various types of controllers discussed in Section VI-B are designed and tested the example system to evaluate their effectiveness. Wind data from the National Renewable Energy Lab’s EWITS study are used. The simulation covers a 30-day period, and the controller commands update every 5 minutes. Each controller is designed with the appropriate level of information: controllers that use exact future knowledge are given the entire wind power trace ahead of time, stochastic controllers are given the probability distribution (39) for the test period, and the other two controllers are given no future information.

For each controller type, a number of different controllers are designed with varying values of the penalty  $\alpha$  (31) or the hysteresis threshold  $\beta$  in (41). This yields a range of controllers of the same type with varying attributes. The results are shown in Figure 8. The horizontal axis shows the number of capacitor switches. The vertical axis represents total STATCOM usage, measured as cumulative absolute value  $\sum \text{abs}(\bar{S})$ . As our optimization goal is to minimize both capacitor switching and STATCOM usage, the best performance is found in the lower left of the plot.

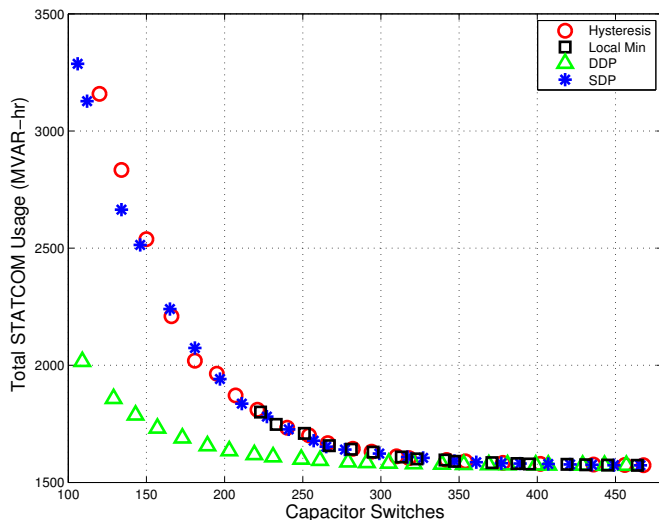


Fig. 8: Performance of various types of optimal controllers based on different types of information. Best performance is attained with low STATCOM usage and low capacitor switching, in the bottom left of the figure. These data are for one month periods. Detailed time traces are shown in Figure 9.

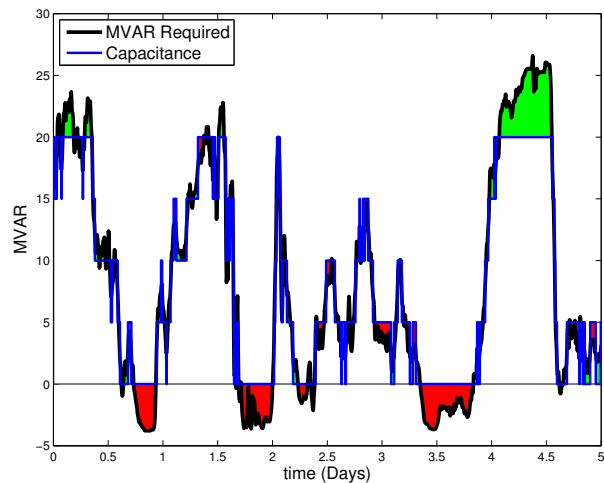
#### D. Discussion

The DDP controllers designed with perfect information demonstrate the best performance, which is to be expected. Perhaps more surprising is that the other three controller types all generate similar performance. This motivates an open research question: What level of future information is appropriate? For the five information classes enumerated in Section VI-A, the two simplest cases (classes 4 & 5) yield similar performance, but the most complex case (class 1) yields vast improvements. This points to a “middle ground” of controller complexity, where significant improvements may be found with reasonably complex controllers of classes 2-4. If exact future knowledge provided no benefit, simple controllers could be used while attaining optimal performance.

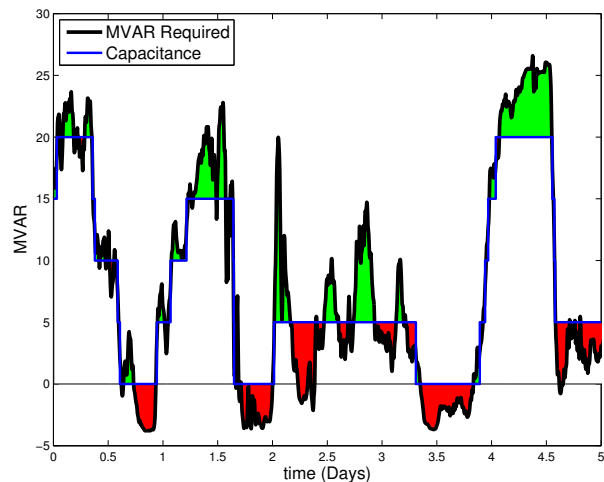
The IO controllers generate identical performance to the baseline hysteresis method because they essentially do the same task. With no future knowledge, the instantaneous optimization is based solely on the cost function (31). A capacitor switch will not occur until the STATCOM usage exceeds the cost of the capacitor switch, which acts as a threshold policy. Arguably, the simple hysteresis method is a rudimentary optimization.

The behavior of the instantaneous optimization has a discontinuity, as shown by the unpopulated gap in capacitor switches. At each time step, the STATCOM usage is evaluated for only that time step. The maximum savings of switching in one capacitor bank is finite, specifically the value of the capacitor bank times the time step. If the cost of a capacitor switch exceeds this maximum, no capacitors will ever be switched on because the decrease in STATCOM usage is always less than the cost of a capacitor switch.

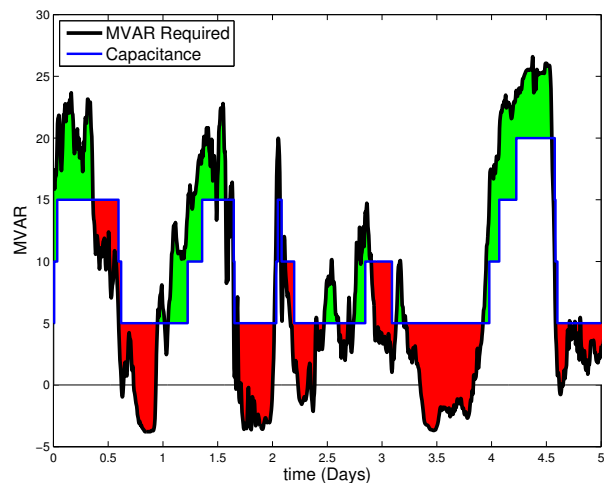
The performance of the SDP stochastic controllers is identical to that of the simpler controllers without any future



(a) Minimum STATCOM/max switching case for Dynamic Programming with exact future knowledge.



(b) Moderate switching (98 Switches) with Deterministic Dynamic Programming and exact future knowledge.



(c) Moderate switching (98 Switches) with Stochastic Dynamic Programming and future statistics. knowledge.

Fig. 9: Time traces of wind farm reactive power control. The solid black line is the required reactive power, the solid blue line is the capacitance and changes in discrete steps with the switches. The green and red regions represent the positive and negative STATCOM usage required to exactly meet the reactive power demand.

knowledge. This implies that the Markov chain wind model used does not provide any additional future information. This is clear from the calculated statistics (39) as the distribution of change in wind power is approximately constant regardless of the current wind power. The SDP controllers studied here use a very simple Markov chain wind model. More sophisticated controllers can be designed that use additional states and generate better performance, for example by storing the last few wind power values rather than just the current value. They will still be classified as having stationary stochastic knowledge (class 4). Markov chains are not particularly good at wind forecasting [6].

Although the example system used here is very simple, the optimization framework of Section VI-A1 can handle very complex systems. Additional attributes [7] may be considered including reserve requirements, failure probabilities, capacitor discharge times, short and long term STATCOM limits, etc. The downside of this framework is computation, which typically grows exponentially with the number of system states. Including all the equipment in a substation is feasible, including all the equipment in a region is probably not. These techniques can provide the most benefit for systems with complex dynamics, constraints, non-intuitive behavior, and a relatively small number of actuators ( $< 15$ ). Large problems can often be partitioned [8], [9] with some loss of optimality, i.e. solving for the reactive power output of each substation, then solving for the reactive power supply within each substation to meet that requirement.

## VII. CONCLUSIONS

The control of reactive power support for wind generation is a challenging problem on several levels. WTGs themselves may be used to provide reactive power support, but the design of the collector system may limit their reactive power output as demonstrated on an example system.

Two cases of low-level system stability were analyzed, highlighting the difficulty of incorporating multiple types of equipment with independent SISO controllers together to form a cohesive unit. In one case, capacitive susceptance causes a tap-changing transformer to change voltage gain - the high side voltage decreases with increasing tap ratio. In a second case, the active controllers for a tap changing transformer and a reactive current source interact to create an instability. Even for devices that may be stable on their own, under certain conditions they can interact and yield unexpected behavior.

System-level considerations also play a role and optimization methods can be important. Various types of controllers were used to control the reactive power support in a substation. These controllers all had varying levels of future information: some had perfect prediction, some had stochastic predictions, and some had no information. The results demonstrate that future knowledge plays an important role in determining optimal solutions, but rudimentary future knowledge in the form of simple wind forecasts based on Markov chains provide no additional benefit. This leaves an open research question about the role of forecasting in these systems, and the relative tradeoff between controller complexity and performance as more and more information becomes available.

## REFERENCES

- [1] E. H. Camm, M. R. Behnke, O. Bolado, M. Bollen, M. Bradt, C. Brooks, W. Dilling, M. Edds, W. J. Hejduk, D. Houseman, S. Klein, F. Li, J. Li, P. Maibach, T. Nicolai, J. Patino, S. V. Pasupulati, N. Samaan, S. Saylor, T. Siebert, T. Smith, M. Starke, and R. Walling, "Reactive power compensation for wind power plants," in *Proc. IEEE Power & Energy Society General Meeting PES '09*, 2009, pp. 1–7.
- [2] —, "Wind power plant substation and collector system redundancy, reliability, and economics," in *Proc. IEEE Power & Energy Society General Meeting PES '09*, 2009, pp. 1–6.
- [3] —, "Characteristics of wind turbine generators for wind power plants," in *Proc. IEEE Power & Energy Society General Meeting PES '09*, 2009, pp. 1–5.
- [4] D. Bertsekas, *Dynamic Programming and Optimal Control Vol 1*. Athena Scientific, 2005.
- [5] —, *Dynamic Programming and Optimal Control Vol 2*. Athena Scientific, 2005.
- [6] K. Brokish and J. Kirtley, "Pitfalls of modeling wind power using markov chains," in *Power Systems Conference and Exposition, 2009. PSCE '09*, 2009.
- [7] I. Erlich and H. Brakelmann, "Integration of wind power into the german high voltage transmission grid," in *Proc. IEEE Power Engineering Society General Meeting*, 2007, pp. 1–8.
- [8] A. Tapia, G. Tapia, and J. Ostolaza, "Reactive power control of windfarms for voltage control applications," *Renewable Energy*, vol. 29, p. 377392, 2004.
- [9] J. L. Rodriguez-Amenedo, S. Arnalte, and J. C. Burgos, "Automatic generation control of a wind farm with variable speed wind turbines," *IEEE Transaction on Energy Conversion*, vol. 17, no. 2, pp. 279–284, Jun. 2002.